

DESIGN AND ANALYSIS OF A THERMOACOUSTIC HEAT ENGINE

Henry Griscti¹, Jordan McPeake¹, Bradley Scott¹ and Carl Howard¹

¹School of Mechanical Engineering
The University of Adelaide, Adelaide SA 5005, Australia
Email: carl.howard@adelaide.edu.au

Abstract

Thermoacoustic heat engines (TAEs) are a well-established technology, however practical applications are limited. TAEs operate when a temperature gradient is applied that causes acoustic oscillations. This paper presents a tutorial on how to design and build a TAE. Focus is given to the design process and analysis of the TAEs performance in order to describe how it was developed and provide a standard to which future TAEs can be assessed.

1. Introduction

A thermoacoustic heat engine (TAE) is a device which relies on an applied temperature gradient to drive a thermodynamic cycle and convert heat energy into acoustic work, producing a sound wave.

A TAE consists of two heat exchangers and a stack inside a resonance tube. The stack consists of a series of parallel channels bounded by a ceramic material. It is the component where the thermoacoustic cycle takes place. Heat is introduced to the system and transferred to the working fluid from a hot heat exchanger (HHX). This heat transfer results in a temperature increase of the working fluid, and the associated pressure increase forces the fluid through the stack to the cooler region. Heat is then transferred out of the system, from the fluid to the cold heat exchanger (CHX), causing a decrease in temperature and thermal contraction. As the temperature of the fluid decreases so does its pressure, and the fluid returns to the beginning of the cycle. This cycle is repeated, and the oscillation of the fluid inside the stack produces work in the form of a sound wave. The work produced in this sound wave is then transferred to the resonance tube (an air column), creating a longitudinal standing-wave [1]. Figure 1 shows a basic schematic diagram of a TAE and its main components.

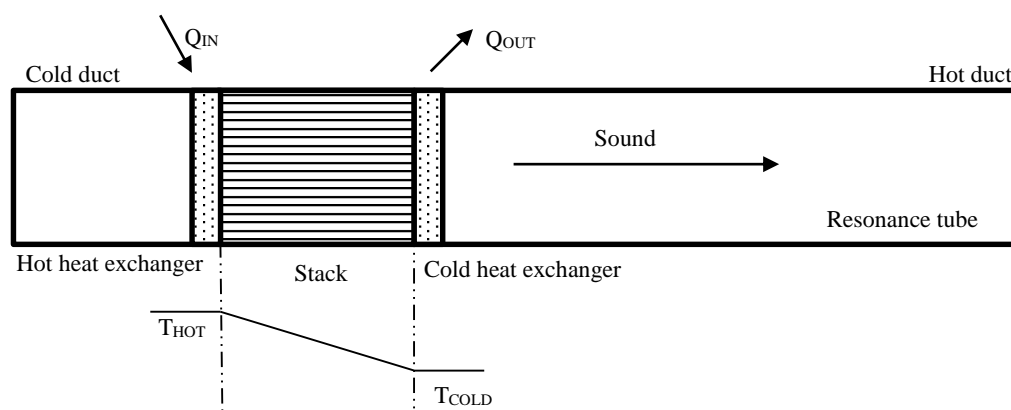


Figure 1. Standing wave TAE schematic diagram.

The development and manufacture of the TAE in this work was undertaken in order to allow experimentation and analysis into phase, frequency, and amplitude control of the generated sound wave. This paper is presented as a tutorial, explaining the engineering design process used to successfully design, build, and test a TAE.

The following sections detail the design method, including computer simulations and mechanical design to develop the TAE. Experimental aims, instrumentation and procedures are described for the tests undertaken. The experimental results are discussed and the future work of the project is outlined.

2. Development & Computer Modelling

The development process of the TAE included initial feasibility research, computer simulation in the low amplitude thermoacoustic modelling program DeltaEC, and mechanical design for the TAE system. The computer model was developed to theoretically test the design of the engine before manufacturing.

2.1 DeltaEC

The DeltaEC software [2] was used to conduct design studies of the proposed TAE. The name DeltaEC is an acronym for ‘Design Environment for Low-amplitude Thermo-Acoustic Energy Conversion’. A model of the proposed engine design was developed in DeltaEC to verify the operation, evaluate the performance, and calculate expected outcomes for the physical engine.

The core design of the model was developed in accordance with certain physical specifications, as discussed in section 3.1, and once the operation was verified, certain variables were changed in order to assess how these variables affected the output. This included the geometric variables, such as stack length and position, duct lengths, heat exchanger size, heat input, and temperatures. The operating points of the final design are indicated on the graphs with an X.

The DeltaEC software uses “targets” and “guesses” to create set points that must either be met (targets) for a program run to be successful, or which are flexible or allow the program to find where the system will work (guesses). These topics are explained in the DeltaEC user’s guide (p. 82 of version 6.3b11) [2], and available online at www.lanl.gov/thermoacoustics.

The position and length of the stack has significant effects on the sound level generated. The stack should be placed in a position closer to a pressure antinode, rather than a velocity antinode [3]. This reduces losses due to viscous shear, which is dependent on gas velocity amplitude [4]. A useful function of DeltaEC is the ability to increment the input variables and plot the effect it has on results. Design studies were conducted to determine the effect of the stack position on the generated sound level; the total length of the TAE was held constant, and the ratio of cold duct length to hot duct length was varied i.e. as cold duct length increases, hot duct length decreases the same amount. The actual numerical values of sound pressure level (SPL) in Figure 2b are not of interest, but rather the change of SPL caused by the position of the stack.

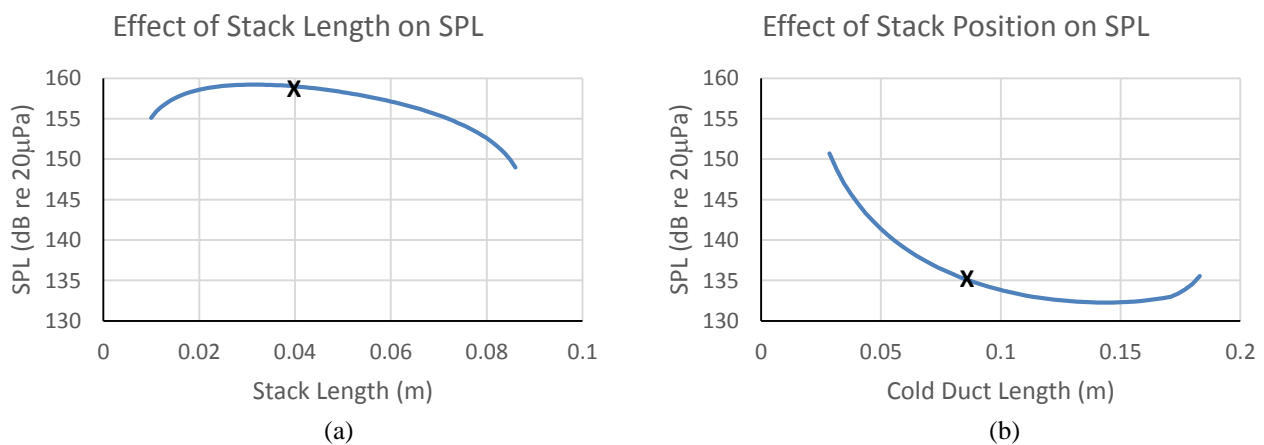


Figure 2. Effect of stack length and position on SPL; (a) stack length is varied and all other variables are held constant; (b) position of the stack is varied by changing the ratio of cold to hot duct lengths, all other variables are held constant.

Figure 2a shows how the length of the stack has an effect on the SPL. If the stack length is too short, there is inadequate space to allow the thermoacoustic effect to work at optimum potential. As the stack length is increased to a value greater than the optimal length, which in this case is 30mm, the difference between the temperatures of the hot and cold ends must be increased to maintain the temperature gradient.

The heater element used in the physical TAE was a nichrome wire that was modelled in DeltaEC as a parallel finned heat exchanger, with a width equal to the wire diameter. The dimensions of the hot heat exchanger model were developed using measurements of the stack material shown in Figure 3, the wire diameter, and appropriate approximations. The stack cross section was measured and photographed using an Olympus BX60M microscope.

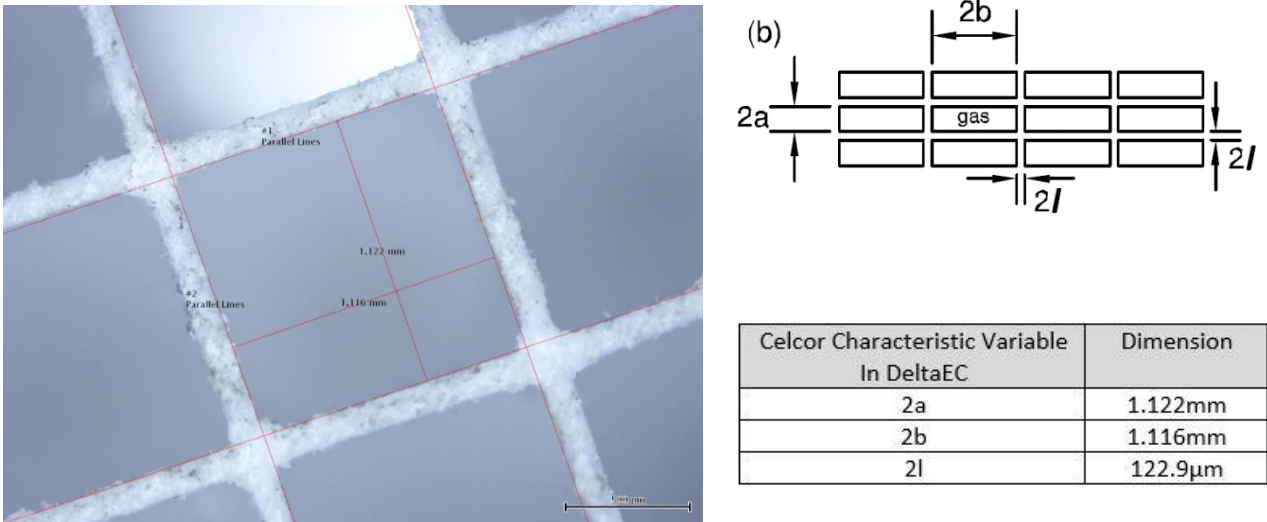


Figure 3. Microscope image of Celcor and dimensions of the pore sizes of the Celcor material.

The CHX is a parallel finned heat exchanger which was designed and manufactured specifically for this project. The DeltaEC model was used to assist and evaluate the design of the CHX. The variables of the design were limited by material and manufacturing constraints. For the simulation, a target was set that the temperature of the fins would remain at 17°C.

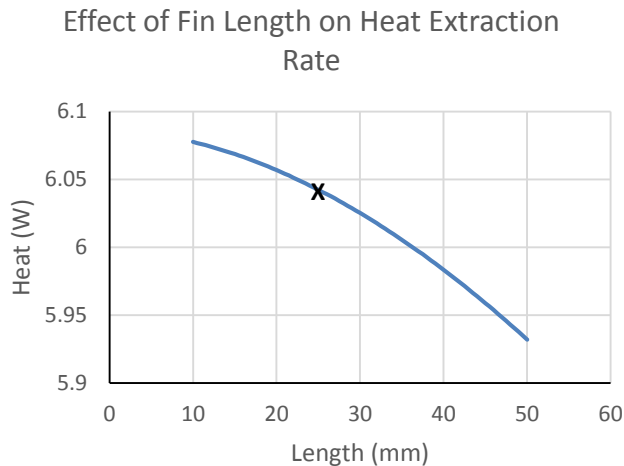


Figure 4. Effect of cold heat exchanger fin length on heat extraction rate. The fin length is varied while keeping all other variables constant.

Due to the simplified DeltaEC model used to simulate the TAE, the results found approximate indicators of the actual performance of the engine; as such an experimentally measured value within 20% of the predicted value was considered a successful outcome.

3. Mechanical Design

The TAE mechanical design was based on the results of the computer simulation combined with material, manufacturing, and operational requirements. Figure 5 shows an annotated cross sectional drawing, and a photograph of the manufactured TAE. The design of the components is discussed below.

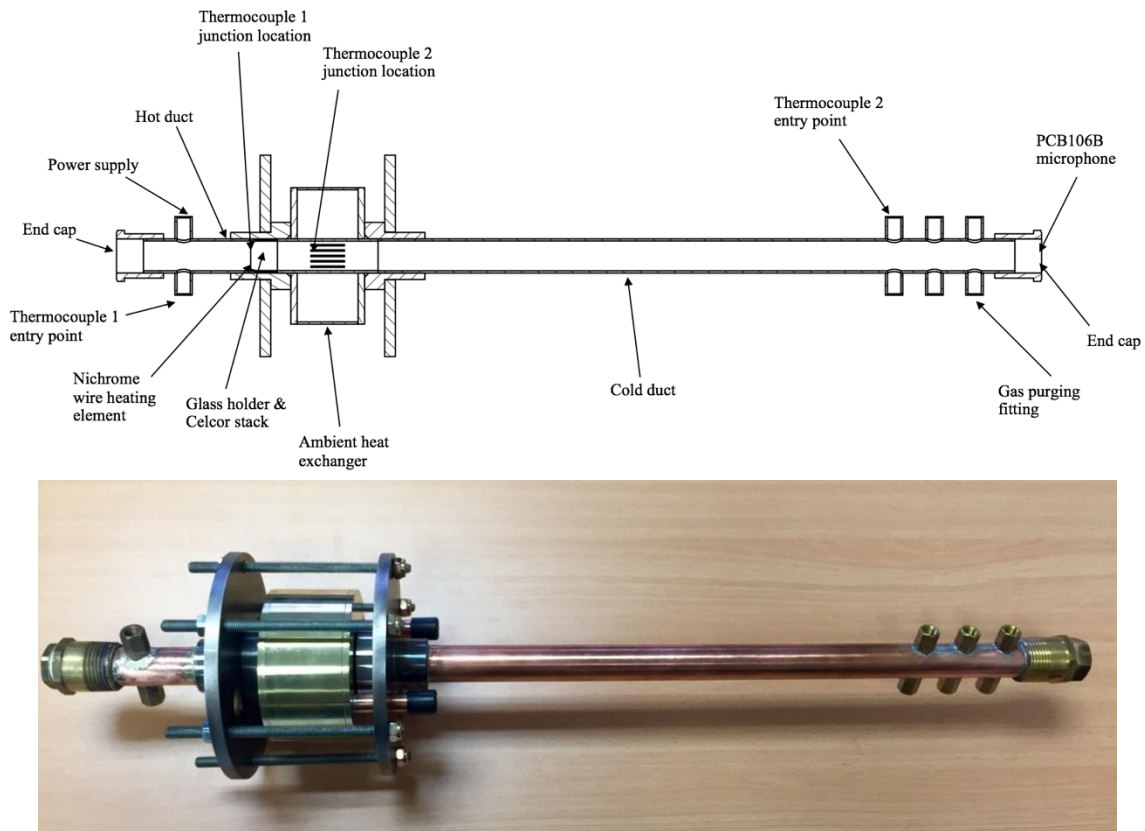


Figure 5. Thermoacoustic heat engine; top: annotated cross section drawing; bottom: photograph of manufactured TAE.

3.1 Design requirements

Some of the design challenges of TAE were the selection of materials to accommodate high temperatures, the access and placement of sensors, and the need to be able to assemble and disassemble the TAE. The constraints addressing these challenges are shown in Table 1 below. These design constraints were relevant to the requirements of the experimental processes and were separate from the more technical constraints developed from mathematical theory and thermoacoustic modelling.

3.2 Design method

After defining specifications and constraints, the concept development phase began. This involved creating multiple concepts and assessing which satisfied the design constraints, and the selection of appropriate materials.

3.3 Design finalisation & construction

Below is an explanation of the key components in the TAE. Particular focus is given to the justification of various design attributes.

- **Resonator:** The resonator constitutes the main body of the TAE. It is constructed from the hot and cold ducts, and end caps. It is required that the end caps are able to accommodate a range of sensors, and must also provide a gas-tight seal. One inch copper tubing was chosen to construct the cold and hot ducts because it is readily available and can be easily soldered. The 1 inch outer diameter was a nominal value, chosen due to ready availability from suppliers and its ease of integration of other standard parts.

Standard 1 inch brass bushes and caps were chosen for the end caps because they were readily available for purchase from local suppliers. The inner diameter of 1 inch allows them to fit around the copper tube and their brass composition allows for easy soldering of these two components. The end cap consists of an outer permanently connected bush, and a threaded inner cap. The inner cap is replaceable with custom made sensor mounts.

Table 1. Constraints and their relative importance.

Constraint	Relative Importance
Ease of assembly/ disassembly	Easy assembly and disassembly is crucial as the system will need to be taken apart many times to allow for the replacement of components, changing and inspection of heating elements, and insertion of various sensors.
Ease of access for sensors and power supply	To properly analyse the TAEs performance, many sensors must be placed inside. A power supply must also enter the system. As a result, it is constrained that the system design should allow for easy access placement of these sensors.
Gas tight	The working fluid within the TAE will be varied to analyse the performance of the TAE under different conditions. Implicit in this constraint is the requirement of an efficient method of filling the system with different gases.
Heat-proof electrical isolation	The nichrome heating element used in the TAE will reach high temperatures (in excess of 450°C). At these temperatures common plastic wire insulation will melt.
Consistent and uniform resonator cross section	The thermoacoustic effect is sensitive to obstructions or changes to the cross section along the resonator tube. Therefore, efforts must be made to minimise any obstructions or deviations from the nominal resonator diameter.

- *Sensor Ingress:* Brass bosses were joined to both the hot and cold ducts to allow access for sensors, power cables, and argon. These brass bosses have an internal thread into which Swageloks and gas taps can be secured. Argon enters through a gas tap and exits via an open endcap acting as a vent. The argon is purged through the system for a sufficient time that guarantees all air has been removed. Swageloks provide a simple and robust method of inserting the thermocouples and ensuring a gas tight seal.
- *Cold Heat Exchanger:* The CHX uses a number of fins which transfer heat from the hot gas inside the resonator to water flowing in the surrounding jacket. The water is pumped from a reservoir, through the water jacket, and then returned to the reservoir to be recycled.
- *Stack & Hot Heat Exchanger:* The mechanical design of both the stack and HHX are very simplistic. The stack is made of a cylindrical section of Celcor, carefully machined to the correct dimensions. Celcor is commonly used because of its uniform geometry, ease of shaping, low cost and high availability [3]. As the heat source for the engine is an electrical resistance heater, this also doubles as the HHX. The hot heat exchanger/element is made of a single nichrome wire. These two components are combined in the hot heat exchanger-stack assembly by bending the nichrome wire into channels cut into the end of the Celcor stack, this is shown in Figure 6. This arrangement positions the hot heat exchanger precisely at the end of the stack and creates minimal obstructions to the airflow within the resonator. The electrical resistance of the nichrome heating element at room temperature was 1 ohm, and this increases with temperature.

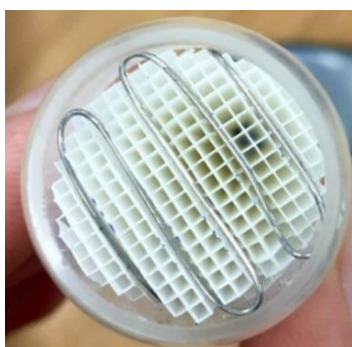


Figure 6. Top view of the hot heat exchanger, stack and glass holder assembly.

- *Glass Holder:* The hot heat exchanger-stack assembly is held inside an adapted glass test tube. The electrical resistance heating element reaches high temperatures and as a result, it must be held in a component of a non-conducting material with a high heat resistance. Therefore, an appropriate material for this is glass. A test tube shape is also suitable as it fits easily into the copper duct, and its rounded end stops the hot heat exchanger-stack assembly from passing into the hot duct.
- *Assembly Method:* The TAE is assembled using a flange and compression technique. Each end of the resonator has a flange attached to it, and the CHX is placed between them. The flanges are then connected with assembly bolts and the system is compressed to create gas tight seals around the CHX.

4. Experimental Method

The analysis of the TAE included a variety of tests, including pressure testing, testing at a range of temperatures using both air and argon as the working fluid. The temperature and pressure data was recorded for post experimental analysis. For the sake of brevity, only the results for testing in air are presented in this paper.

To ensure the manufactured TAE met the gas tight design specifications, the entire system was pressure tested using water, at 200kPa (2 bar) for 48 hours and no leaks were detected.

To measure the performance of the TAE, two types of sensors were used. To measure the sound pressure level a PCB106B pressure sensor was used, located at the cold end of the resonance tube. This sensor was housed in a machined component that was easily removable from the device. Two type K thermocouples were used to calculate the temperature difference. The thermocouples were located either side of the stack, as shown in Figure 5. In order to retain the gas tight seal of the system, Swageloks and stainless steel sheathed thermocouples were used. Fibreglass sheathed thermocouples were originally used; however they were swapped for the stainless steel as they didn't provide a sufficient gas tight seal.

The data was acquired using a National Instruments CDAQ 9188, with analogue input and thermocouple input modules. The data acquisition hardware was connected to a computer and the data was recorded and analysed using NI SignalExpress 2014.

The power wires had to be electrically isolated from each other and the rest of the engine, and also able to withstand temperatures exceeding 450°C. Uninsulated wires were used to connect the nichrome heating element, as the available plastic or silicone based insulation on wires was not rated to these expected operating temperatures. Ceramic sheaths and fibreglass sleeving was investigated to isolate the power wires, and as the fibreglass sleeve was considered less intrusive it was used. The wires entered the system via a specifically designed boss in the hot duct and were sealed using a black silicone adhesive to 'plug' the entry hole while still remaining electrically isolated.

5. Results & Discussion

5.1 DeltaEC comparison

Analysis of the experimental results allows a direct comparison of the actual performance of the TAE with the performance predicted by DeltaEC. Table 2 shows a number of important parameters and their predicted and experimental values. Comparisons of most significance relate to actual and predicted resonant frequency and SPL at a given temperature difference. These comparisons show that the TAE performed above expectation, and that the simulation provided a conservative, yet valid performance prediction. The accuracy of the DeltaEC model can be increased by improving the model, especially with respect to acoustic losses caused by experimental equipment obstructions.

DeltaEC calculated the resonant frequency of the TAE by numerically integrating functional acoustic equations. Actual frequency was measured by a pressure sensor placed at the cold end of the resonator tube. At the set temperature $T_1 = 400^\circ\text{C}$ the simulation predicted that the TAE would operate a frequency of 271 Hz while it actually operated at 247 Hz. This gives a difference of 24 Hz and an error of 9% of the predicted value. An error of 9% shows that the simulation provided a very accurate prediction. Differences in the results are due to the transition from model to 'real life' and any error less than 10% is a significant achievement. This result shows that DeltaEC provides an accurate simulation

of TAE engine frequency. However, if it is crucial that the TAE operate a specified frequency, this program would not be suitable.

Table 2. DeltaEC parameters with corresponding predicted and experimental values.

Parameter	Measured Value	DeltaEC Prediction
Heating element temperature, T_1 (°C)	400	400
Air temperature between cold heat exchanger and stack, T_2 (°C)	54	38
Temperature difference across the stack, ΔT (°C)	346	362
Maximum RMS sound pressure P_{max} (Pa)	2576	1904
Maximum sound pressure level (dB) $P_{ref} = 20\mu 6$	162	160
Operating frequency, f (Hz)	247	271

The SPL provides an indication of how powerful the TAE is, SPL is dependent on the potential difference created by the temperature difference. At a hot heat exchanger temperature of 400°C it was predicted that the SPL would be 160 dB, with the actual pressure level being 162 dB. This gives a difference of 2 dB and correlates to a 26% increase with respect to predicted maximum RMS sound pressure. An error of over 25% is significant, however this is a successful result for the TAE as it shows that performance has exceeded expectation. Figure 7 displays SPL vs temperature difference with series for predicted and experimental values. The results show that the TAE was able to generate a higher amount of acoustic pressure from a given temperature difference than was predicted.

This could be because of the difference between the actual and modelled hot heat exchanger geometry. Due to the approximations made, the hot heat exchanger used in the experiment was larger than that which was modelled. As a result, the electrical power needed to heat the greater amount of resistive wire was increased and hence, the rate of heat transfer from the hot heat exchanger also increased. The larger heat exchanger provided more energy to the thermoacoustic cycle and therefore increased the SPL. In essence, the analysis of SPL demonstrates that the rate of heat transfer and heat exchanger temperature should both be simulated as accurately as possible to provide accurate predictions of acoustic performance.

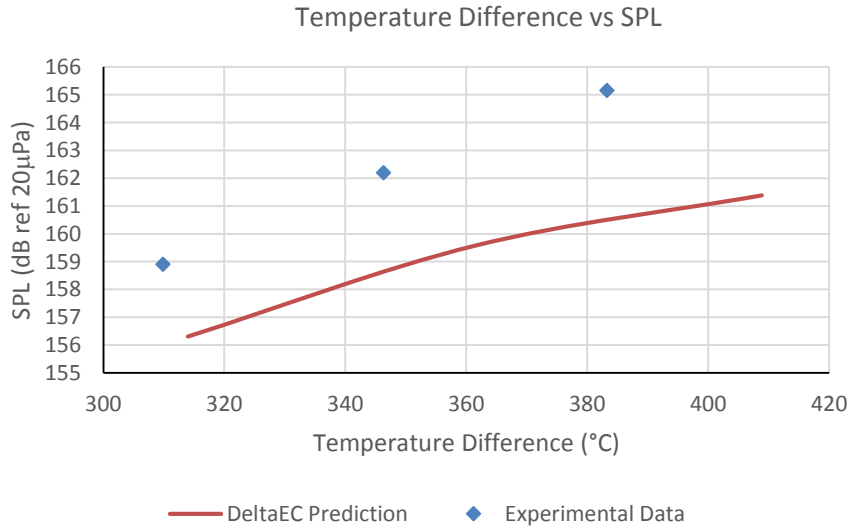


Figure 7. Comparison between measured data and DeltaEC prediction of temperature difference over the stack vs SPL.

5.2 Pressure amplitude

The relationship between pressure amplitude and temperature difference was well observed and provides great insight into the TAE’s performance. Figure 8b show a plot of pressure amplitude and temperature difference vs time. This figure details the operation of the TAE throughout a complete experiment. The plot can be split into five key sections to assist the analysis. These sections include the: start of the

experiment, heating phase, initiation of the thermoacoustic cycle, amplification of the sound wave, and termination of the experiment.

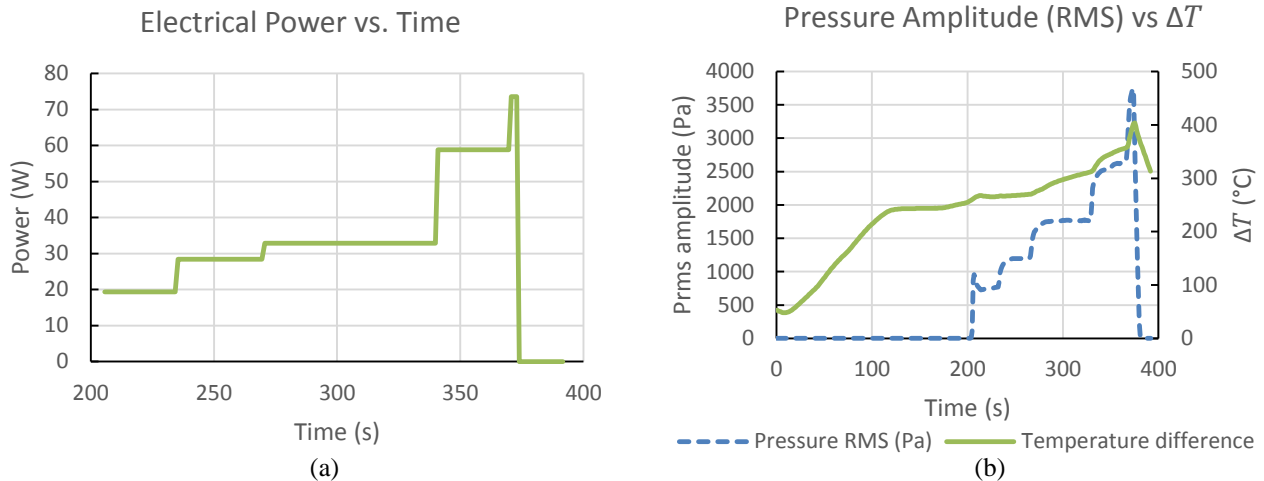


Figure 8. Experimental data in air; (a) Electrical power input over time; (b) RMS pressure amplitude vs temperature difference over the stack.

- **Start:** At $t = 0\text{ s}$ the pressure amplitude is at ambient level ($<20\text{ Pa}$) and the temperature difference is very low. It would be expected that the temperature difference would be 0°C at the start of the experiment, but due to previous operation of the TAE, the heating element was still warm and the temperature difference was around 50°C .
- **Heating Phase:** The heating phase takes place between the initial application of current to the heating element and the initiation of the thermoacoustic cycle. The recording of the data began slightly before the application of current to the heating element; this is why the temperature difference is decreasing for the first 5-10 seconds. Throughout the heating phase the pressure amplitude remains at ambient level and is distorted. This is a clear indication that the thermoacoustic cycle is not operating. To begin, the temperature difference rises quickly, from around 40°C at 5 seconds to 240°C at 120 seconds. The temperature then plateaus as the applied current is slowly increased in the period preceding the initiation of the thermoacoustic effect, from 120 seconds to 200 seconds.
- **Initiation:** The thermoacoustic effect is initiated when ΔT equalled 261°C . This is referred to as the critical temperature difference. The time taken to establish a stable cycle is approximately 5 seconds. In this short period, the pressure amplitude increases from $<20\text{ Pa}$ to approximately 1000 Pa.
- **Amplification:** The amplification period following the establishment of the thermoacoustic cycle sees the pressure amplitude increase as more power is applied the heating element to increase the temperature difference. The amplification period sees the pressure amplitude increase from 1000 Pa to 3750 Pa, relating to a rise in ΔT from 260°C to 400°C . As expected during the amplification period, a rise in temperature difference causes a rise in the pressure amplitude. However, the plot shows an interesting response from the pressure amplitude to an increase in the temperature difference. The response between pressure and temperature appears to be roughly linear over the entire data range. However, the pressure curve is comprised of 'steps', whereas the temperature curve changes more gradually and consistently. The 'steps' in the pressure curve are sections where a rapid increase in pressure is followed by a period of little to no increase. The differences in the curves are due to the different response times of the thermocouple and pressure sensor which were used. As seen in Figure 8a, the power is increased in steps. This means that the heating element temperature will also rise in steps. However, the thermocouple cannot accurately track a rapid increase in heating element temperature due to its own thermal inertia. This means that the pressure amplitude is more responsive to temperature increase than is shown in Figure 8b. Further analysis would benefit from the use of a more responsive thermocouple.
- **Termination:** The amplification operation of the TAE is terminated when ΔT reaches 400°C . This was to ensure that the heating element and other internal components were not damaged by excessive heat. Operation was terminated at 375 seconds causing a rapid decline in the temperature difference and return of the pressure amplitude to ambient conditions.

5.3 Temperature plot

The temperature plot shown in Figure 9a describes the operation of the two heat exchangers. The hot heat exchanger performed as expected. The use of a simple resistance heating element for this device provided a high level of temperature control and reliability. The heating element was quick to respond to a large power increase at the start of each experiment. It was then able to maintain a constant or slightly increasing temperature during the operation of the cycle when greater accuracy was required.

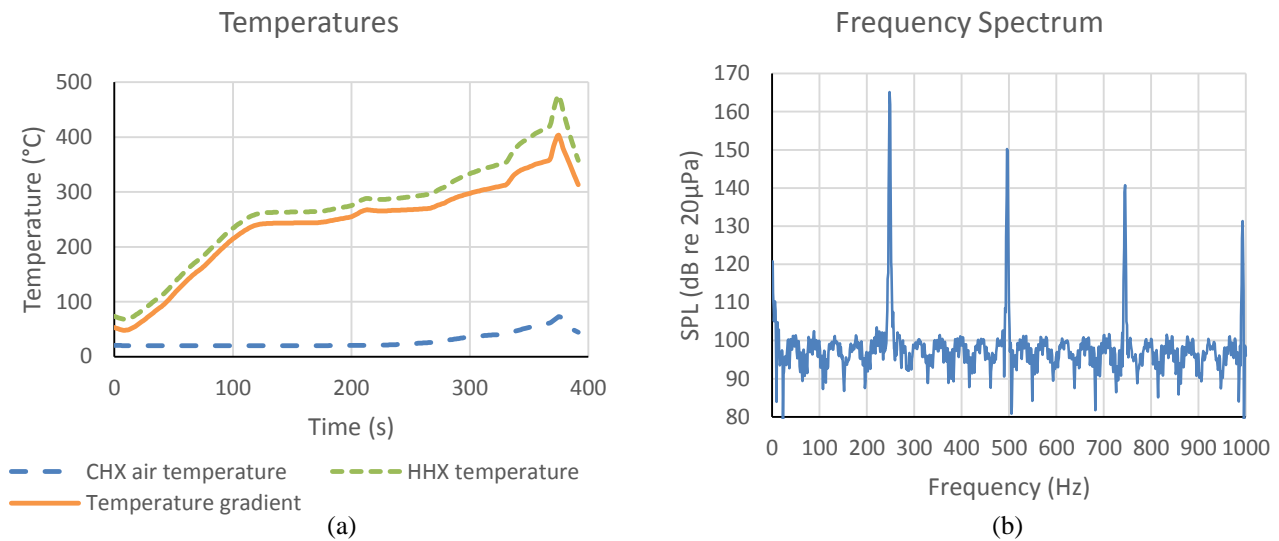


Figure 9. TAE experiment results; (a) temperature of the hot and cold ends of the stack, and the difference between the two; (b) frequency spectrum of the TAE operating with air, and $T_1=450^{\circ}\text{C}$.

Figure 9a shows that the CHX also performed to a high standard. The CHX was able to maintain the cold end of the stack at its initial temperature for over 240 seconds. This is impressive, considering the hot heat exchanger was operating at over 250°C only 40mm away. After 250 seconds, the cold temperature begins to rise, eventually reaching approximately 75°C . The water used as the cold fluid in the heat exchanger was supplied at ambient temperature. As a result of this, heat transfer within the heat exchanger only operated across a small temperature difference. To increase the rate of heat transfer it would be suitable to reduce the temperature of the cold fluid by adding ice to the water reservoir. This would be a simple and effective way of improving the performance of the CHX.

5.4 Frequency spectrum

The frequency spectrum of the TAE's sound wave at $T_1 = 450^{\circ}\text{C}$ is shown in Figure 9b. It can be seen that the frequency spectrum presents defined peaks and uniform regions of low SPL. The primary 247 Hz tone is dominant, with harmonics at 497 Hz, 746 Hz and 995 Hz also very prominent.

5.5 Limitations & possible improvements

The success of this TAE has led to the realisation of some significant limitations and possible improvements to the TAE and experimental designs. Limitations of this experiment relate to the recording of the electrical power used and acoustic power produced by the TAE. Data on these two parameters would be helpful in improving the understanding of the TAE and would allow one to assess efficiency. It is envisioned that provisions will be created to allow for the measurement of these parameters. Further improvements also include the ability to vary the frequency of the TAE by adjusting the resonator length, and controlling the phase of the sound wave by a number of different methods.

6. Further Work

A conventional TAE is able to produce a high amplitude sound wave; however, there has been no mention of phase control in any research literature. The further work of this project is research and experiment with methods of increasing control of the output sound wave; this includes phase, amplitude and frequency control of the output sound wave. Increase in sound wave control may make TAE technology suitable for high temperature active noise control.

7. Conclusion

This paper has described an engineering design process that was used to successfully design, build and test a TAE. The experimental results exceeded the predicted performance. The measured operational frequency was within 9% of the predicted value using the DeltaEC model, while the TAE produced a SPL of 2dB greater than predicted. Some of the experimental limitations included recording the electrical power supplied and the acoustic power produced. Further work involves modifications to the device to enable the control of the phase, amplitude and frequency of the generated sound wave.

Acknowledgements

The authors would like to acknowledge and thank David Gardner, who played a major part with the initial development and design of the thermoacoustic heat engine; and OptoFab for their contribution of the machining and preparation of the glass holder. This work was performed in part at the OptoFab node of the Australian National Fabrication Facility utilising Commonwealth and SA State Government funding.

References

- [1] Swift, G. *Thermoacoustics: A unifying perspective for some engines and refrigerators*, Acoustical Society of America, Melville, New York, 2002.
- [2] Ward B., Clark J. and Swift G. *Design Environment for Low-amplitude Thermoacoustic Energy Conversion DELTAEC Users Guide*, Los Alamos National Laboratory, Version 6.3b11, 2012.
- [3] Liu J., Garrett S.L., Long G.S. and Sen A. "Separation of thermoviscous losses in Celcor™ ceramic", *Journal of the Acoustical Society of America*, **119** (2), 857-852 (2006).
- [4] Hariharan, N.M., Sivashanmugam P. and Kasthuriangan S. "Influence of stack geometry and resonator length on the performance of thermoacoustic engine", *Applied Acoustics*, **73** (10), 1052–1058 (2012).